# Experimental Facility and Measurement Technique for Study of Scattering Properties of Conductive Objects in its Near-Field Zone

Yuri I. Belov, Ivan A. Illarionov[1]

*Abstract* – **Double-antennas EHF AM transceiver measuring system (TRX MS) for to measure signals scattered by objects, when the system is situated in its near-field zone, is briefly described. Physical Optic (PO) simulation of the radar system and experimental measuring of signals scattered by the conductive sphere of 30 wavelengths diameter, which were measured in distances to the sphere from ~ 10 up to 2000 wavelengths are presented and discussed.**

*Keywords* –**transceiver bistatic measuring system, RCS in near-field zone, avoid collision systems**

## I. INTRODUCTION

Radar detection of objects in its near-field zone (i.e. where the objects cannot be presented as point sources) as well as study of the EM waves scattering against a distance to the illuminated objects is a significant interest for various radar applications: a military one – proximity fuse CW sensors [1], also a civilian one – radar avoid collision systems for tower cranes, cars, helicopters [2], as well for the near field-far field (NFFF) antenna measuring systems, see, e.g., [3].

Use of the EHF range for radar systems operating in the object's near-field zone permits to diminish the TRX and its antennae overall dimensions, while technology progress of the electronic components production makes the EHF systems more and more cheap. In real situations the objects, which are avoided to collide, as a rule, will be illuminated not completely because the EHF aperture-type antennae provide high directivity. Consequently the scattering objects could be structured in a set of simple (elementary) components like plane, sphere, and cylinder; it makes easier the computer simulations and understanding of scattering processes in the objects near field zone.

To determine the RCS of objects by processing of its scattered fields measurements in the near-field zone commonly is used "classic" bistatic radar technique, see one of the publications on the subject [4]. The technique naturally restricts the angle range, where the scattering parameters of objects in its far-zone are determined. It is the angular vicinity of the collimated beam or main beam of radiating antenna of the measurement facility, which imitates plane wave in some area [5].

Yuri I. Belov is with Radio Physics Research Institute, Bolshaya Pecherskaya Str, 25/12a, 603950, Nizhny Novgorod, Russia, belov@nirfi.sci-nnov.ru
Ivan A. Illarionov is with the State Technical University, Minina Str, 24, 603950, Nizhny Novgorod, Russia, illarionovi@list.ru

Along with the bistatic radar technique to determine the RCS by the monostatic technique it is widely used the "inverse synthetic aperture radar" (ISAR) method of various its modifications: spherical waves (SW) ISAR [6], image based (IB) NFFF transformation [7].

The very remarkable fact been noted in [7] is that a backscattering differential RCS of some simple (elementary) shape object (a cone of 10 wavelengths) with a spherical bottom been studied), which was measured by the IB NFFFT technique in its near-field zone without special processing has a value approximately the same as the correct backscattering RCS (a difference is less than 5 dB and dependent of the incident wave polarization as well of the distance up to the object). Similarly the same relation is observed between the RCS in the near-field zone (let call it further like "quasi-RCS") and the far-field zone RCS in [8], which were evaluated for circle and square plane disks.

As the mentioned cone, as well the plane disks are the simple shape objects. If there are several of them in an illuminating radar antenna beam, it is necessary to take into account its common input into received signal, like it has been suggested in [9] by the next algorithm.

For the scattering centers of complex targets (a set of simple objects), which do not change its positions during radar illumination, RCS of the target is squared complex sum of signals reflected by every scattering center. The relative phases of signals are determined by appropriate delays counted from a reference point:

$$\sigma = \left| \sum_{m=1}^{M} \sqrt{\sigma_m} \exp\{i 2 k_0 z_m \cos\frac{\beta}{2} + \xi_m\} \right|^2 , \qquad (1)$$

where the $\sigma_m$ – is RCS of the m–numbered scattering center, $z_m$ – is a projection of spatial displacement (relatively to the reference point) of the m-numbered center point to the bisectrix of the bistatic angle β (the angle between an incident ray from radiating antenna and a reflected ray to receiving antenna), $\xi_m$ – auxiliary phase factors for the model (i.e., propagation fluctuations), $k_0 = 2\pi/\lambda$ , $\lambda$ – wavelength.

If to replace in (1) inputs of the separate RCS components $\sqrt{\sigma_m}$ by the quasi-RCS values evaluated or measured in the objects near-field zone, the procedure to estimate the RCS of a complex object will be essentially easier and faster.

Our experimental study of behavior of the quasi-RCS for the simple shape object – the sphere of 30 wavelengths diameter – has been conducted along a broad range of distances from the sphere vertex up to the plane of aperture

horns which were used in the developed radar been described in this paper.

The developed experimental radar system uses the quasi-monostatic technique (two horns, radiating and receiving, separated by a distance ca 70 mm in H-plane) for the purpose to increase dynamic range and realize a possibility to make measurements in very near-field zone (from distance of 0.5 ÷2.0 diameters $D_{sph}$ of the sphere ).

It was recognized, in the simulations and in the experiment, that evaluation accordingly to introduced in [10] value the RCS-I, that is termed the "quasi-RCS" in our terminology shows: if a ratio of the radar received power to transmitted power, to multiply by 4-th degree of distance «*r*» to target (sphere), the result will present smoothly oscillating function against the distance. This is true for the ratios $m = \frac{r_{ff}}{r}$ ( $r_{ff} = \frac{2D_{sph}^2}{\lambda}$ is the far-field distance) from 1 up to 20, see Figs. 3 and 5.

Mathematical model of the quasi-bistatic radar as a set of dipoles situated in the near-field zone of a spherical conductive target was developed. It has used the Physical Optics (PO) approximation of currents on the sphere with taking into account a shape of windowing for every source point of the radiating and receiving antenna, see (10) below. Further, a computational estimate of the windows shape impact showed a weak influence of the non-uniform component surface current evaluated in the Physical Theory of Diffraction (PTD) approximation. The impact study was implemented for the sphere of 20 wavelengths diameter and λ = 1 cm similarly to the technique developed in [11]. The result is presented in the Fig. 7.

The problem of experimental study of the RCS of various objects in it's the near-field zone against of distance (including the automatically detection of the objects) could be split in two parts. First one is to design a simple and reliable measuring system for to use it in any natural conditioned experiments. Second one is to develop effective techniques for to measure RCS of the studied objects and its structural components in its near-field zone with a reasonable values of reflections from facility surrounding the objects.

As been told above, it is rationally to develop a structure of the measuring system as well known anti-collision CW radar with bistatic sounding mode.

In the paper we present a brief description of the CW radio AM transceiver measuring system (TRX MS) supplied with double antennas in close (~10 wavelengths) proximity and which is intended to measure received signal in the object's near-field zone [12]. Some peculiarities of data processing technique to separate an impact of echoes scattered by the rotator supporting objects, as well some experimental results on the topic are discussed.

To analyze the experimental data and to arrange the directions of investigation program it was suggested a simple model of scattering objects (sphere and circular disk) in the PO approximation, which was used to simulate signals radiated and received by the bistatic radar system with the aperture type antennae.

The measurements of signals received by the TRX MS from metallic sphere of 30 wavelengths diameter situated in distances from 10 up to 2000 wavelengths were conducted, the results are presented in Figs. 3 and 4; it were compared with the computed radar model. The received signals in any distance up to the sphere vertex were multiplied by 4-th degree of the distance. The impact of clutter is clear recognized in the Fig.3 for longest distances. The signals received from the round plane disk 30 wavelengths diameter against it aspect angles are presented in Fig. 7 as the sample of a recognized target with known RCS, which was influenced with a remarkable background clutter.

## II. Experimental Facility

Double-antennas radio transceiver measuring system (TRX MS) [12] is situated on the adjusting unit which provides transfer of the system in 3 Cartesian coordinates as well as azimuth rotation for the system pointing. The TRX MS consists of the transmitter (TX), receiver (RX), ADC/DAC converter (USB-module) and power supply (battery) module. Microwave CW signal of the transmitter is modulated in amplitude by low frequency (meander mode), which is selected by the narrow band amplifier of the receiver, thus it increases sensitivity of the receiver.

The TX unit is jointed with the transmitting antenna input. The basis of the TX is waveguide Gann oscillator with the invar stabilizing resonator. The nonreciprocal waveguide ferrite is used for stabilizing and isolation of the oscillator. The ferrite is jointed with the p-i-n diode modulator creating the meander modulation mode; further microwave power is transferred in the main arm of the directional coupler.

A part of generated power is branched off by the directional coupler in secondary arm, which is loaded by the low-voltage broadband waveguide detector to check the oscillator operating power. On this aim the AM signal is digitized in the USB unit and sent to the control PC. The main part of the microwave signal via the directional coupler, in its turn, is separated into the signal part for compensating clutter signals in the RX (similarly it was done in [13]), and the second part of signal going through the p-i-n diodes attenuator to radiating antenna. The last part of the power is digitally controlled via the USB unit by an industrial PC.

Antenna unit consists of two similar horn antennae: transmitting – TA, and receiving − RA one, both with the aperture sizes 32x21 mm, which are separated in ca 70 mm between of its axes in H-plane. Antennae gains are ~ 20 dB, beam width is ~ 10º in – 3 dB power level. To point the horns to the studied objects there is a small diode laser between antennae with beam collinear to its axes.

RX unit is the CW receiver with two amplifier stages of 40 dB gain, which are jointed via a ferrite; the last amplifier is loaded by the waveguide detector. Sensitivity of the receiver is less than minus 90 dBm.

Output of the detector comes to the LF amplifier of 40-50 dB gain.

ADC/DAC unit with the USB-unit provides a transforming of AM meander voltage of the reference and measuring channels into codes and further transfers the codes

to the small industrial PC. The DAC channel is used to control the TX output power with the p-i-n modulator by means the manually generated code. The received signal is automatically recalculated by the PC to the so called "spatial attenuation" [dB] my means of the table of preliminary calibrating measurements of a standard attenuator, which were conducted by the TRX MS. The "spatial attenuation" is dB decreasing of received signal relatively to the transmitter power in the radiating antenna input.

The experiments technique used largely the methods described in [13]. That was the choice to simplify the TRX MS and to keep a good sensitivity of the facility. The rotator of the TRX MS serves to point the antenna complex to the central point of calibrating testing objects (spheres and discs). The rotator of the tested objects allows a varying of aspect angles and maximizing the received signal in calibrating process. A record of received signal against of the TRX shift along the sounding direction permits to evaluate average power of the complex sum voltages due to reflections from studied object and from the supporting it rotator, as well the power of the signal reflected by the rotator only (the target should be deleted). The compensating system of the TRX MS permits to exclude the clutter signal made by the object rotator for a single distance to the TRX MS. The studied object, as it is shown in [13], should not to disturb the clutter structure of the certain experiment. We conducted all experiments in the large anechoic chamber.

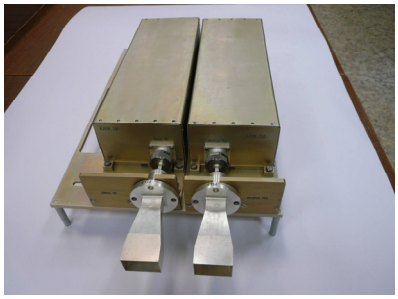

Fig.1. Experimental radar front-end facility

## III. Simulation Model of Measurement Procedure

The mathematical model of the bistatic radar system was developed to analyze experimental results and to determine the basic direction of future investigation program.

In the model the TA and RA were presented as the sets of electric dipoles which were used for to reduce the calculation time, because the expression of radiated magnetic field, which determines the surface current on the scattering object, is simpler, than for magnetic dipoles sources.

The antenna patterns of arrays consisted of electric or magnetic dipoles are very similar except the vicinity of $\vartheta \approx 90^{\circ}$, thus the used TA (as well as RA) model is universal enough.

Electric fields in the near-field zone for the Cartesian coordinate system are presented by the next expressions:

$$\vec{E}(x,y) = F \cdot \sum_{n',m'} (\vec{I}^{e}_{n'm'} P(r) - Q(r)(\vec{I}^{e}_{n'm'} \cdot \vec{r}_0)\vec{r}_0) \frac{e^{-ikr}}{4\pi r} \qquad (2)$$

where $F = \frac{-iW_0 2\pi}{\lambda} \Delta xa \cdot \Delta ya$; $W_0$ – impedance of free space; $\Delta xa, \Delta ya$ –are the space intervals between discrete source currents; $\vec{I}^{e}_{n'm'}$ – are the complex magnitudes of electric currents with numbers *n'*, *m'* of the modeled antenna array.

The current orientations as well as its spatial distribution are being chosen by an investigator in the simulation process. We used *y* polarization in the model:

$$\vec{I}^{e}_{n'm'} \cdot \vec{y}_0 = I^{e}_{n'm',x} = \left| p_{xy}(xa_{n'}, ya_{m'}) \right| \cdot \exp\{i\varphi_{xy}(xa_{n'}, ya_{m'})\},$$

$xa_{n'}, ya_{m'}$ – are the Cartesian coordinates of a dipole on the TA aperture with indexes $n' = 0, \pm 1, ...N'; m' = 0, \pm 1, ...M'$.

$$P(kr) = 1 + \frac{1}{ikr} - \frac{1}{(kr)^2} \qquad (3)$$

$$Q(kr) = 1 + \frac{3}{ikr} - \frac{3}{(kr)^2} \qquad (4)$$

$$kr = \frac{2\pi}{\lambda}\sqrt{(x - xa_{n'})^2 + (y - ya_{m'})^2 + z(x,y)^2},$$

$\vec{r}_0 = \vec{r}/|\vec{r}|$ – is the unit observation vector.

Accordingly to chosen aperture currents polarization the radiated magnetic fields are: $H_y(x,y) = 0$,

$$H_x(x,y) = \frac{1}{i2\lambda} \cdot \sum_{n',m'} \left[ I^{e}_{n'm',y} \cdot C(r) \cdot \frac{z(x,y)}{r} \right] e^{-ikr} \Delta xa \cdot \Delta ya \qquad (5)$$

$$H_z(x,y) = \frac{-1}{i\lambda} \cdot \sum_{n',m'} \left[ C(r) \cdot I^{e}_{n'm',y} \cdot \frac{(x - xa_{n'})}{r} \right] e^{-ikr} \Delta xa \cdot \Delta ya \qquad (6)$$

$$C(r) = 1 + \frac{1}{ikr} \qquad (7)$$

The terms of order $\frac{1}{(kr)^2}$ in coefficients *P* and *Q* were neglected in the fields' simulation for reduction of the evaluation time. Amplitude and phase distributions of the aperture fields on both antennae models were specially evaluated in electromagnetic simulation of the horns of the experimental facility.

The basic integral equation to calculate the fields scattered by an elementary conductive objects *S* is the expression of the electric vector potential being formed by the surface current $\vec{J}_s$, which in its turn is determined accordingly to the PO approximation:

$$\vec{A}(\vec{r}) = \mu \iint_S \vec{J}_S(\vec{r}\,') G(|\vec{r} - \vec{r}\,'|) dS' \qquad (8)$$

$$\vec{J}_s = 2\vec{n} \times \vec{H}_{\tau inc}, \qquad (9)$$

where $G(|\vec{r} - \vec{r}\,'|) = \frac{1}{4\pi|\vec{r} - \vec{r}\,'|} e^{-ik|\vec{r} - \vec{r}\,'|}$ – free space Green's function, $\vec{H}_{\tau inc}$ – is the tangential component of the incident magnetic field, $\vec{r}\,'$ – scattering surface current point vector.

The expressions for the scattered fields are similar to the Eqs. (2) – (7) and used to calculate the scattered fields. A shadowing of some elements for both antenna array models was taken into account, when they were in near-zone of the conductive sphere been used as a scatterer. For this aim the geometrical optic (GO) technique has been implemented. The equation for the boundaries of visible areas (spatial filter) for the radiating and receiving element arrays $x = xa_{n'} = d; y = ya_{m'} = b; z = 0$ could be written as:

$$\left[x - \left(\frac{a}{z_0 + a}\right)^2 d\right]^2 - \left(\frac{a}{z_0 + a}\right)^4 d^2 + \left[y - \left(\frac{a}{z_0 + a}\right)^2 b\right]^2 - \left(\frac{a}{z_0 + a}\right)^4 b^2 + \left(\frac{xd + yb}{z_0 + a}\right)^2 = a^2\left[1 - \left(\frac{a}{z_0 + a}\right)^2\right] \quad (10)$$

where $z_0$ is the coordinate of the sphere vertex, which is the nearest to the antenna array apertures; $a$ is the radius of scattering sphere.

It should to remark, that the shadowing been taken into account as the GO technique is remarkable for distances up to the sphere vertex only less than 20 wavelengths. When a conductive disk is used as a target, the shadowing is obviously absent.

In aperture of the receiving array the x-component of electric field is summed for every dipole and the squared its result is considered as the received antenna power. It is evaluated for various distances up to scattered object as well as for various aspect angles.

In Fig. 2 there are shown (as squire dots) the results proportional to the power been integrated (summed) in the aperture of receiving model array (32 x 21 sq. mm.). It was evaluated along the described mathematical model. The scattering object was the conductive sphere of 30 wavelengths diameter; polarization field of both modeled antennas was linear.

The model was corresponded to the described facility and scattering object parameters been used in the experiments.

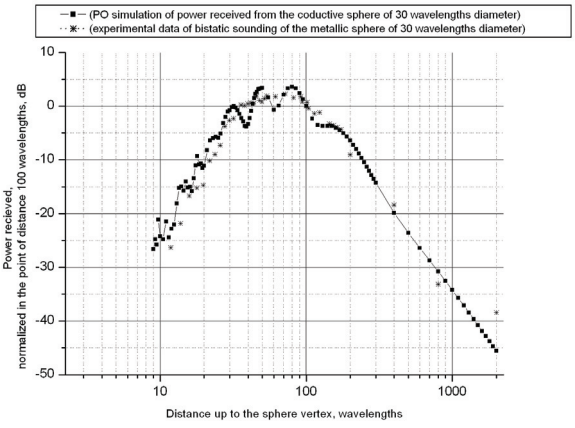


Fig. 2. PO modeling and experimental results for sounding the sphere of 30 wavelengths diameter

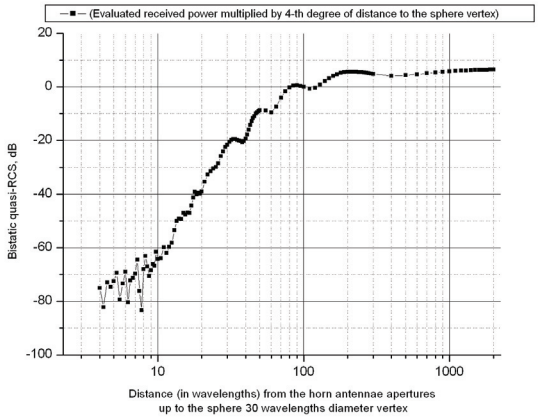


Fig.3. Evaluated (shown in Fig.2) received power in the near-field radar model multiplied by 4-th degree of distance from the radar antennae apertures up to the sphere vertex

## IV. Experimental Results

In the Fig. 4 it is shown the spatial attenuation (see its characterization in the section II) normalized by the transmitter power. The attenuation is proportional to the received power of developed bistatic radar system, when it was measured in the near-field zone of the conductive sphere of 30 wavelengths diameter. The distance between the TRX MS and the target from 10 up to 2000 wavelengths was changed consequently and the attenuation was measured.

It is easy to understand that nearly of the studied spherical target (~30 wavelengths or the sphere diameter) received signal increases, on a reason of increasing the illuminated target area (10). In the near-field zone the beam divergence does not prevail to increasing of the solid angle relevant to the illuminated area, but at more far distances (near of 3 sphere diameters) the spherical (proportional to $1/r^2$) divergence of the both antennae fields reduces the received signal.

A comparison of the experimental results with the computer simulation in Fig.2 shows good similarity, but not completely, because the model did not take into account the interaction of transmitting antenna and the sphere (VSWR modulation, see illustration of the interaction in the near-field zone on Fig.4), as well as the signal scattered by target rotator, which was not excluded because the compensation procedure [13] takes too long time for the whole measurement data set. Really the PO model does not correctly describe the currents on the sphere in the object nearest field zone [14], but when we have compared the fields been scattered by a sphere with the surface currents in PO approximation as well as with taking into account the non-uniform surface PTD component evaluated along the technique developed in [11], the results are very similar, see the Fig. 7.

In Fig.5 the received signal to be multiplied by 4-th degree of distance thus determining the RCS1 [10] value achieves the far-zone RCS in a distance ca of six the sphere diameters. Also remarkable variations could be seen in the curve for the great values of argument show an impact of clutter, i.e. comparatively large value of noise in measured signal. The background signal level estimates could be taken from Fig. 8 further, where the signals received from the circular disk of

diameters 30 wavelengths (at the distance 9 meter) against aspect angles are presented.

Conditions of experiment which has been conducted with the circular disk were that the object was put in the rotator with the RCS great enough, thus the target was being recognized, when attenuation decreased more than 10 dB during change of the aspect angles. The rotator with the disk was situated in 9 m far away from TRX MS, i.e. in the far zone of every disk.

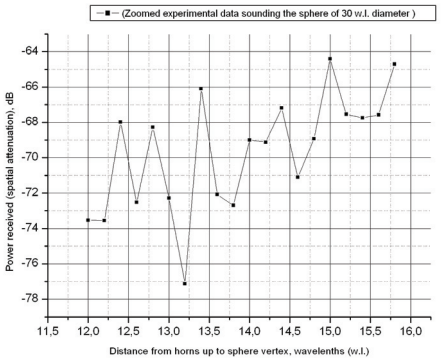


Fig. 4. Zoomed experimental results for sounding the sphere of 30 wavelengths diameter

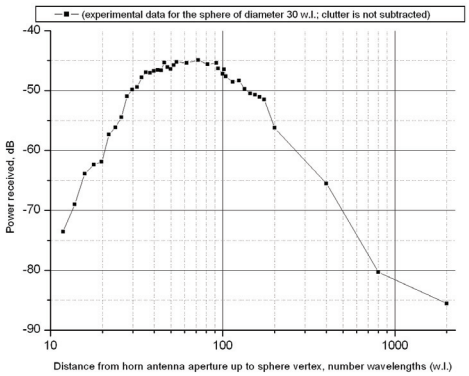


Fig. 5. Experimental results for sounding the same (as Fig. 3) sphere for 12 – 2000 wavelengths distance

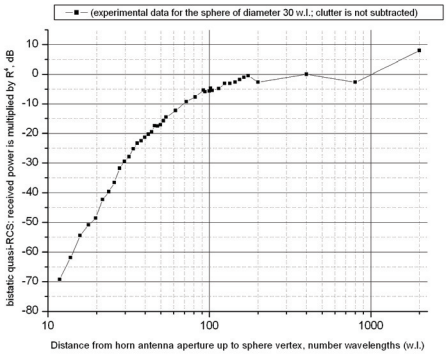


Fig. 6. Data shown in Fig.4 multiplied by 4-th degree of distance from the horns up to the sphere vertex

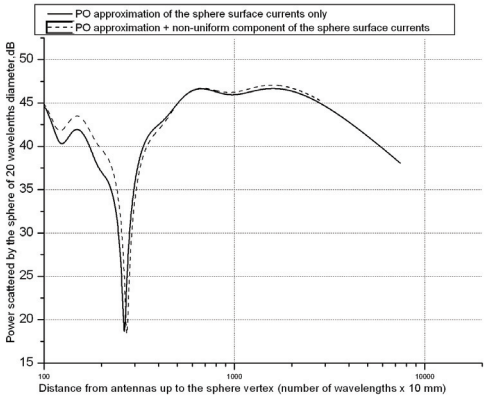


Fig.7. Power scattered by the conductive sphere 20 wavelengths diameter along the distance from the sphere vertex up to the point observation on the axis coming through the sphere center

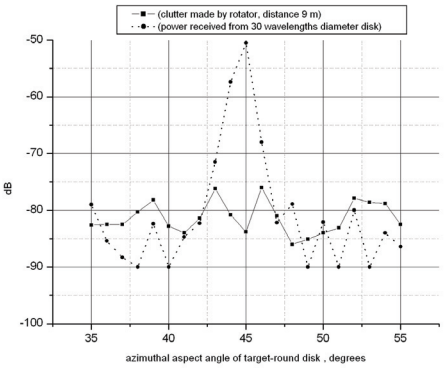


Fig. 8. Experimental detection of circular disc of 30 wavelengths diameter at 9 m distance by the TRX MS against aspect angle

These measurements with a set of discs and spheres of various diameters implemented by the TRX MS placed in its far zone have provided the calibration procedure in which the measured spatial attenuation was recalculated into RCS values. The set of 7 calibrating spheres and disks supplied the accuracy of RCS calibration ± 3.6 dB

## V. CONCLUSIONS

It is evident that, there is a great statistical variety of the bistatic RCS of real objects in its near-field zone as a function against shape, distance, aspect angle of scattering objects, thus the study of the problem is not completed, but some basic results of the presented work could be formulated as the next one.

The first result. The measurements of spatial attenuation been conducted with real studied calibrating objects (disks and spheres) by the developed TRX MS facility, provides as a result the requested dynamical range of sensors in the objects near-field zone, for example, for avoid collision systems. The calibrating objects as the simple shape targets were studied from the *far zone distance up to the distance of diameter of the object.* The measurements errors produced by an impact of the fields scattered by the studied objects and produced by the surrounding medium were estimated.

The second result. The bistatic configuration of the radiating and receiving horns will permits to use the developed experimental TRX MS for purposes to analyze the scattered fields of not only passive scattering objects, but also by the scatterer with a load (i.e. antenna), thus to study an antennae interaction during the measurements of antenna parameters in its near-field zone.

The third result. The quasi-RCS of real complex objects could be studied as a combination (complex sum (1) with the weights of the quasi-RCS) of scattered signals from the simple shape components in its near-field zone.

## ACNOWLEDGMENT

The author is very grateful to Mrs. S. Chernikova, Mr. S. Miniev, Mr. A. Repin, Mr. N. Skipetrov, Mr. A. Tikhonov for essential assistance in arrangement of the facility, conducting of the experiments and fruitful discussions.

## REFERENCES

[1] *Radar Handbook*, editor-in-chief M. I. Skolnik, 2-d edition Mc Graw-Hill, 1990.

[2] R.N. Bates, A.G. Stove "Millimetre-wave radar", *Philips J. Res.*, vol. 41, no. 3, pp. 206 -218, 1986.

[3] Yu. I. Belov, I.A. Illarionov, E.L. Varentzov, "Experimental study of radiation patterns of the open-end rectangular waveguide placed near conductive objects", *Magazine "Antennas"*, pp. 18 -27, issue 12, 2010, (in Russian).

[4] T. B. Hansen, R. A. Marr, U. H. W. Lammers, T. J. Tanigawa, and R. V. McGahan **"**Bistatic RCS Calculations From Cylindrical Near-Field Measurements—Part I: Theory*"*. *IEEE Trans. on AP-S,* vol. 54, No. 12, pp.3846 -3856, Dec. 2006.

[5] Daniel Zahn, Kamal Sarabandi. "Near field Measurements of Bistatic Scattering from Random Rough Surfaces*"*, *URSI/IEEE AP-S Int. Symposium, 2000.*

[6] Broquetas, J. Palau, L. Jofre, and A. Cardama. "Spherical Wave Near-Field Imaging and Radar Cross-Section Measurement", *IEEE Trans. on AP*, vol. 46, no. 5, pp. 730 – 735, May, 1998.

[7] I.J. LaHaie. Overview of an Image-based Technique for Predicting far-Field RCS from Near-Field Measurements*. IEEE AP Magazin*e, no.6, pp. 159 – 169, Dec. 2003.

[8] C. Bourlier, Ph. Pouliguen. "Useful analytical formulae for near-field monostatic RCS…". *IEEE Trans. on AP*, vol. 57, no.1, pp. 205 –214, Jan. 2009.

[9] R.E. Kell, "On the derivation of bistatic RCS from monostatic measurements," *Proc. IEEE*, vol. 53, pp. 983-988, Aug. 1965.

[10] J.M. Taylor and A.J. Terzuoli, " On the concept of near field radar cross section", presented at *IEEE AP-S Int. Symp.* Canada, pp. 1172-1175, July 13-18, 1997.

[11] T.B. Hansen, and R. A. Shore "Incremental Length Diffraction Coefficients for the Shadow Boundary of a Convex Cylinder". *IEEE Transaction on AP*, vol. 46, no.10, pp. 1458 – 1466, Oct. 1998.

[12] Yu. Belov, S. Minejev, A. Tikhonov. "Measurements of bistatic RCS in the objects near field zone". *Proc. of Int. conference IST-2010*, Nizhny Novgorod, 2010 (in Russian).

[13] O.P. McDuff, H. Mott and C.S. Durrett, Jr., "Backscattering measurements of slowly moving target", *IEEE Trans. on MTT*, vol.12, no. 5, pp. 541-546, Sept. 1964.

[14] P. Ya. Ufimtsev, *Theory of Edge Diffraction in Electromegnetics*. Moscow, Publ. Co. "Binom", 2007 (in Russian)